Anti-cancer activity of di- and tri-organotin(iv) compounds with D-(+)-Galacturonic acid on human tumor cells.

Anti-cancer activity of di- and tri-organotin(IV) compounds with D-(+)-Galacturonic acid on human tumor cells

Alessandro Attanzio[a], Maristella Ippolito[a,1], Maria Assunta Girasolo[a], Filippo Saiano[b], Archimede Rotondo[c], Simona Rubino[a], Luigi Mondello[d], Massimo L. Capobianco[e], Piera Sabatino[f], Luisa Tesoriere[a,*], Girolamo Casella[g,h,*]

[a] *Dipartimento di Scienze e Tecnologie Biologiche Chimiche e Farmaceutiche (STEBICEF), Università degli Studi di Palermo, Parco d'Orleans II, Viale delle Scienze, Edificio 16, 90128 Palermo, Italy*
[b] *Dipartimento di Scienze Agrarie, Alimentari e Forestali, Università degli Studi di Palermo, Parco d'Orleans II, Viale delle Scienze, Edificio 4, 90128 Palermo, Italy*
[c] *Dipartimento di Scienze Biomediche, Odontoiatriche e delle Immagini Morfologiche e Funzionali- Università di Messina, A.O.U. Policlinico "G. Martino" Via Consolare Valeria, pad. G, Torre biologica, 98125 Messina, Italy*
[d] *Dipartimento di Scienze Chimiche, Biologiche, Farmaceutiche ed Ambientali, Università di Messina, Stagno d'Alcontres, 31-98166 Messina, Italy*
[e] *ISOF - CNR Area della Ricerca di Bologna, Via P. Gobetti 101-40129 Bologna, Italy*
[f] *Dipartimento di Chimica "Giacomo Ciamician", Alma Mater Studiorum, Università degli Studi di Bologna, via F. Selmi 2, 40126 Bologna, Italy*
[g] *Dipartimento di Scienze della Terra e del Mare (DiSTeM), Università degli Studi di Palermo, Via Archirafi 10, 90123 Palermo, Italy*
[h] *Consorzio Interuniversitario di Ricerca in Chimica dei Metalli nei Sistemi Biologici (C.I.R.C.M.S.B.), Piazza Umberto I, 70121 Bari, Italy*

A B S T R A C T

We have compared the anti-proliferative activity *in vitro,* of $R_2SnGala$ (**1-3**) [R = Me, n-Bu, Ph] and novel $R_3SnGala$ (**4**, **5**) [R = Me, n-Bu] with D-(+)-Galacturonic acid [HGala; $Gala^{q-}$, q = (2) and (1) for $R_2SnGala$ and $R_3SnGala$, respectively] compounds, towards human tumor cell lines of intestinal carcinoma (HCT-116) and breast adenocarcinoma (MCF-7). The new synthesized **4** and **5** compounds were characterized, in solution, by ^{1}H, ^{13}C and ^{119}Sn NMR, that showed that HGala acts as monoanionic moiety and evidenced the dynamic behavior of the compounds, due to inter-conversions involving the anomeric carbon atom of the ligand. Cell viability, apoptosis induction and cell cycle distribution were analyzed by 3-(4,5-dimethylthiazol-2-yl)-2,5-diphenyltetrazolium bromide (MTT) colorimetric assay and flow cytometry, respectively. The cytotoxicity of the compounds, in the micro-submicromolar range, changed in the order of the organotin(IV) moieties, according to **5** > **3** > **2**, while **1** and **4**, containing $Me_nSn(IV)$ (n = 2,3) moieties, were ineffective. Compound **5** showed peculiar cytotoxic effects. It did not cause time dependent inhibition of cell growth nor accumulated into the cells. Cell death induced by the active **2**, **3**, and **5**, was shown to be apoptotic by measuring the exposure of phosphatidylserine to the outer membrane and the loss of mitochondrial potential. All the cytotoxic compounds induced an accumulation of cells in the subG0/G1phase, while only **2** and **3** perturbed the cell cycle confining viable cells in G0/G1phase. Finally, none of the compounds investigated affected the viability of normal intestinal or liver cells, indicating selectivity towards tumor cells.

1. Introduction

The overcoming of the well-known drawbacks concerning the cisplatin anticancer drugs, *e.g.*, nephrotoxicity, neurotoxicity as well as acquired drug resistance [1], moved the attention to the search of new vicarious metal- and organometal-based drugs [2–8]. In this respect, organotin(IV) derivatives have been widely studied due to their promising activity towards several tumor cell lines [6,7]. To date, it is recognized that the cytotoxic activity of organotin(IV) compounds is exerted by apoptotic mechanisms through different pathways, *e.g.*, interaction with DNA by different binding modes, change in the Ca^{2+} homeostasis, caspase modulation [9,10]. With the aim to modulate the cytotoxicity of the organotin(IV) compounds, a generally pursued strategy is based on the choice of ligands such as: i) drugs, *e.g.* antibiotics, anti-inflammatories, antipyretics, antivirals, to name a few, or ii) small molecules which are involved in metabolic pathways [7,11].

In this context, carboxylate compounds of organotin(IV) are a versatile class of compounds, due to the high stability of the Sn-OCO bond.

* Corresponding authors.
E-mail addresses: luisa.tesoriere@unipa.it (L. Tesoriere), girolamo.casella@unipa.it (G. Casella).
[1] This contribute is part of the graduating thesis of Miss Maristella Ippolito who was member of STEBICEF during her thesis work.

This bond stability allows to choose a suitable ligand in order to tune the organotin(IV) moiety cytotoxicity, including the minimization of unwanted side effects and, thus, they have been extensively studied as anti-proliferative and anti-cancer drugs [7,11–13]. Carbohydrates are ubiquitous in nature and they represent one of the four main classes of macromolecules in biology along with DNA, proteins, and lipids and they are involved in processes such as immune defense, viral replication, cell growth, cell-cell adhesion, inflammation, and signal recognitions [14,15]. Thus, they represent a promising class of molecules to exploit in the field of the organometallic drug chemistry.

For example, it has been observed that carbohydrate-based scaffold ligands tend to easily coordinate active metal centers, also showing some advantages over other ligands, by, *e.g.*, improving the solubility of the compound obtained, lowering undesired toxicity, or enhancing tumor selectivity [16–18].

As far as organotin(IV) chemistry is concerned, the acidic derivatives of carbohydrates, which belong to the class of hydroxycarboxylate compounds, constitute a potential interesting class of ligands to design promising organometallic anti-tumor drugs. Nevertheless, also accounting for the huge diversity of acidic carbohydrates occurring in nature (either in monomeric, oligomeric and polymeric forms), to the best of our knowledge, few works have been reported on the matter [19–27], and, even more, the anticancer activity of organotin(IV) compounds with carbohydrates and their derivatives, has been poorly investigated so far [16,24,25,28].

Among these ligands, D-(+)-Galacturonic acid (HGala; Fig. 1) is a ubiquitous moiety in several biological systems and it is mainly present as a main component of polysaccharides as pectines. These macromolecules showed promising anti-inflammatory and anti-proliferative properties [29–33]. Concerning R_2Sn(IV)Gala compounds, it has been found that in aqueous solution HGala acts as chelating dianionic ligand ($Gala^{2-}$), by deprotonation of a suitable hydroxyl group [$RO^{(-)}$], besides the carboxylic one which acts as first anchoring site [20]. Moreover, in water, organotin(IV) moieties catalyze anomerization equilibria of HGala, by pH dependent mechanism, also increasing the amount of α,β furanosidic forms to the detriment of the α,β pyranosidic ones [23]. In addition the observed kinetic lability of the RO–Sn bond in aqueous medium [23] could also allow the tin to interact with biological targets as cationic moiety. Finally, the interaction of HGala with triorganotin(IV) moieties has not yet been investigated, while complexes with the epimer D-(+)-glucuronic acid have been reported [26,34].

In this work we continue to investigate the anti-proliferative and anti-cancer effect of organotin(IV) derivatives against breast adenocarcinoma MCF-7 and intestinal cancer HCT-116 human tumor cells [35,36] by investigating the potential anti-cancer activity of the title compounds, three of which, $R_2SnGala$ (R = Me, n-Bu, Ph) were already synthesized [20], and two of which are novel $R_3SnGala$ (R = Me, n-Bu) compounds.

2. Experimental

2.1. Synthesis

R_2SnO (R = Me, n-Bu, Ph) were prepared by hydrolysis of the parent R_2SnCl_2 halogenides (gifts from Witco GmbH, Bergkamen, Germany). Me_3SnOH (98%, Alfa Aesar), n-Bu_3SnOCH_3 (97%, Sigma Aldrich) and D-(+)-Galacturonic acid monohydrate ($HGala{\cdot}H_2O$, 97.0%, Sigma-Aldrich) were used without further purification.

2.1.1. Synthesis of $R_2SnGala$ [R = Me (1), n-Bu (2), Ph (3)]

$R_2SnGala$ compounds were synthesized according to the procedure reported elsewhere [20]. $Me_2SnGala$ (**1**) ($C_8H_{14}O_7Sn$): Anal. Found (calc.): C = 28.20 (28.19); H = 4.28 (4.14); Sn = 34.49 (34.82)%; n-$Bu_2SnGala$ (**2**) ($C_{14}H_{26}O_7Sn$): Anal. Found (calc.): C = 39.80 (39.56); H = 5.87 (6.17); Sn = 27.42 (27.80)%; $Ph_2SnGala$ (**3**) ($C_{18}H_{18}O_7Sn$): Anal. Found (calc.): C = 46.86 (46.49); H = 4.08 (3.90); Sn = 25.84 (25.53)%.

2.1.2. Synthesis of $Me_3SnGala$ (4)

2 mmol of Me_3SnOH (362 mg) were dissolved in 20 mL of methanol and then left to react, under refluxing for 48 h, with 2 mmol (425 mg) of HGala. After 48 h, the volume of the solution was reduced under vacuum and an oil was formed. The compound was dried under vacuum, in the presence of P_4O_{10} for 3 days. A white solid was isolated and recrystallized from an acetonitrile/methanol (95:5) mixture. The solution

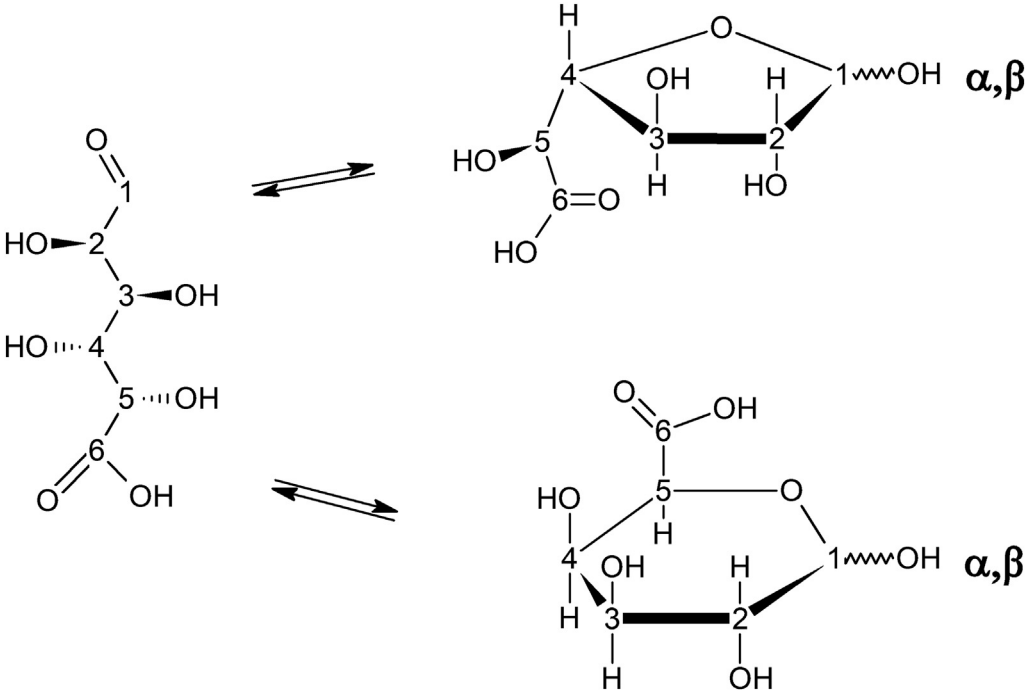

Fig. 1. D-(+)-Galacturonic acid and relevant isomeric/anomeric forms. Top right: furanosidic ring; Bottom right: pyranosidic ring.

obtained was left at 4 °C for 24 h and a precipitate was formed. The precipitate was isolated by filtration, washed with cold acetonitrile (0 °C), and dried under vacuum in the presence of P_4O_{10}. ($C_9H_{18}O_7Sn$) Anal. Found (calc.): C = 29.87 (30.28); H = 5.20 (5.08); Sn = 32.96 (33.26)%.

2.1.3. Synthesis of n-Bu_3SnGala (5)

2.2 mmol of HGala (467 mg) were dissolved in 20 mL of methanol and then left to react under refluxing for 48 h, with 2 mmol (0.58 mL) of n-Bu_3SnOCH_3. After 48 h, the solvent was removed under vacuum and a liquescent oil was formed. It was dried under vacuum for one week, in the presence of P_4O_{10}. ($C_{18}H_{36}O_7Sn$) Anal. Found (calc.): C = 44.32 (44.74); H = 7.53 (7.51); Sn = 24.20 (24.57)%.

2.2. Physical measurements

2.2.1. NMR spectroscopy

NMR spectra were recorded on a VARIAN 500 MHz Magnet equipped with a ONEnmr probe with gradients, coupled with a ProPulse Varian console. All these devices were controlled by a workstation with a linux Centos operating system and running the vNMRj software for the acquisition/processing procedures. All the sample solutions in the 5 mm NMR tubes were between 500 and 700 µL, with concentrations *ca.* 50 mM.

Deuterated solvents were reagent grade (Euriso-top) and they were used as received. Because of their different chemical properties, the methyltin(IV) derivatives, soluble in water, were analyzed in D_2O, while the other compounds were dissolved in DMSO-d_6. According to our preliminary data [23] the water environment induces chemical exchanges between isomeric-anomeric forms, but also between different hydrated compounds, while for the compounds in DMSO-d_6 solution even the exchangeable hydroxyl proton signals of the ligand could be detected.

The 90° pulses were calculated and used for the final 16 scans acquisition with 2.5 s of acquisition time and 2 s of scan delay. The 1D ^{1}H, ^{13}C{^{1}H} and ^{119}Sn{^{1}H} NMR spectra were acquired at 499.74, 125.73, and 186.36 MHz, respectively [37]. 2D spectra, COSY, TOCSY [38–40], NOESY [41], [^{1}H, ^{13}C]-gHSQCAD [42,43] and [^{1}H,^{119}Sn]g-HMBC [44–46] were also acquired in order to achieve a complete assignment of all the species occurring in solution. ^{119}Sn resonances were not always detected in the 1D experiments because of huge line broadening coming from: a) very short relaxation times, b) chemical exchanges involving solvent molecules in the inner and outer coordination spheres (especially for penta and hexa-coordinated species); c) chemical exchange between isomeric compounds. In this context, where needed, {^{1}H,^{119}Sn}-gHMBC spectra without shaped pulses (the old fashioned short-sequence) to detect both the ^{119}Sn resonance and the through-bond possible connections with protons (several more experiments were also run to set up the specific coupling constants) were acquired.

Stability in solution of n-Bu_3SnGala (**5**) *(vide infra)* was investigated on a Bruker Avance II DMX 400 MHz equipped with a 5 mm broad-band BBI probe. One-dimensional ^{1}H and ^{13}C{1H} in DMSO-d_6 and DMSO-d_6/H_2O solutions were acquired at 27 °C with a spectral width (SW) of 12 ppm and 200 ppm, respectively. ^{119}Sn{1H} NMR spectra were recorded at 27 °C with a SW of 200 ppm.

Finally, for ^{119}Sn, Me_4Sn was used as external reference (^{119}Sn, δ = 0.00 ppm). Me_4Si was used as external reference (^{1}H, δ = 0.00 ppm; ^{13}C, δ = 0.00 ppm) for ^{1}H and ^{13}C spectra. LW in the text is intended as line width at half height.

2.2.2. Elemental analyses

The compounds have been analyzed for C and H contents by a CNHS elemental analyzer, mod. FLASH 2000 (Thermo Fisher Scientific Inc.), at the microanalysis laboratory of the University of Padova. Tin content has been analyzed gravimetrically in our laboratories, as SnO_2, by treating the compounds with a HNO_3/H_2SO_4 mixture [47].

2.2.3. ICP measurements

All chemicals used were of ultrapure or of the highest available grade (Merck quality), and all solutions were prepared with ultrapure water (resistivity 18.2 MΩ cm), obtained by a Thermo EASYpureII purification system.

Sn, for the uptake study (*vide infra*) was determined by ICP-MS (Inductively Coupled Plasma-Mass Spectrometry) using an Agilent 7500ce spectrometer equipped with a collision cell, on solutions obtained by microwave digestion of 250 mg of sample dissolved in 3 mL of a HNO_3/HCl = 1:3 solution. The isotope used to quantify the tin amount was ^{118}Sn. Rhodium solution (1 µg/mL) was used as an internal standard.

2.3. Biology

2.3.1. Viability assay in vitro

All the compounds were dissolved in dimethyl sulfoxide (DMSO) and then diluted in culture medium so that the effective DMSO concentration did not exceed 0.1%.

MCF-7 (breast adenocarcinoma), HCT-116 (intestinal carcinoma), Caco-2 (human colorectal carcinoma) and Chang liver cell lines were purchased from American Type Culture Collection, Rockville, MD, USA. All of them were grown in RPMI (Roswell Park Memorial Institute) medium supplemented with L-glutamine (2 mM), 10% fetal bovine serum (FBS), penicillin (100 U/mL), streptomycin (100 µg/mL) and gentamicin (5 µg/mL). Cells were maintained in log phase by seeding twice a week at a density of 3×10^8 cells/L in humidified 5% CO_2 atmosphere, at 37 °C. In all experiments, cells were allowed to adhere overnight and then treated with the compounds or vehicle alone (control cells), whereas Caco-2 cells were treated fifteen days after confluence, at which time the cells are differentiated in normal like cells [48].

No differences were found between cells treated with DMSO 0.1% and untreated cells in terms of cell number and viability.

Cytotoxic activity of the synthesized compounds was determined by the MTT colorimetric assay based on the reduction of 3-(4,5-dimethylthiazol-2-yl)-2,5-diphenyltetrazolium bromide (MTT) to purple formazan by mitochondrial dehydrogenases of living cells [49]. This method is commonly used to illustrate inhibition of cellular proliferation. Monolayer cultures were treated for 24 h with various concentrations (10^{-7}- 10^{-5} M) of the organotin(IV) compounds. Cisplatin was used for comparison. Briefly, cells were seeded at 2×10^4 cells/well in 96-well plates containing 200 µL RPMI. When appropriate, cells were washed with fresh medium and incubated with the compounds in RPMI. After 24-72 h incubation, cells were washed, and 50 µL FBS-free medium containing 5 mg/mL MTT were added. The medium was discarded after 2 h incubation at 37 °C by centrifugation, and formazan blue formed in the cells was dissolved in DMSO. The absorbance, measured at 570 nm in a microplate reader (Bio-RAD, Hercules, CA), of MTT formazan of control cells was taken as 100% of viability. The growth inhibition activity of compounds was defined as the IC_{50} value which represents the molar concentration of the compound that inhibits 50% cell viability. IC_{50} values were calculated using the dose-response inhibition model in GraphPad Prism 5.02 from GraphPad Software (San Diego, CA). Each experiment was repeated at least three times in triplicate to obtain the mean values.

2.3.2. Uptake study

MCF-7 and HCT-116 cells were seeded in triplicate in 24-wells culture plates at a density of 5.0×10^4 cells/cm^2. After overnight incubation, the cells were washed with fresh medium and incubated with compound **5** (0.2 µM) in RPMI. After 6, 24, and 72 h of treatment, the incubation medium was carefully withdrawn and cells, harvested by trypsinization, washed twice with fresh medium. Incubation medium and cells were then submitted to ICP-MS analysis to measure the tin concentration.

Table 1
FT-IR bands (cm^{-1}) for triorganotin(IV) compounds.

Compound	ν(OH)	ν(COOH)	ν_{as}(COO)	ν_s(COO)	Δν	ν_{as} (Sn−C)	ν_s(Sn−C)
$H_2GalA{\cdot}H_2O$	3441vw[a] 3364vw 3320vw	1713vw	–	–	–	–	
4	3387 m	–	1653 ms	1376 m	277	594 m	530 m
5	3387w 3304w	–	1635 ms	1352 m	283	610 s	542 s

[a] s = strong; ms = medium-strong; m = medium; w = weak; vw = very-weak.

Table 2
δ(^{1}H) values (ppm) of all the isomeric/anomeric forms of compounds $R_2SnGala$ [R = Me (**1**), n-Bu (**2**), Ph (**3**)] and $R_3SnGala$ [R = Me (**4**), n-Bu (**5**)]. For **1** and **4**, spectra were acquired in D_2O; for **2**, **3**, and **5**, spectra were acquired in DMSO-d_6.

Compound[a] and its relative amount	H-1	H-2	H-3	H-4	H-5	OH-1	OH-2	OH-3	αCH$_2$	βCH$_2$	γCH$_2$	CH$_3$	Ph
α-[$Me_2SnGalpa$] 15%	5.30	3.80	3.90	4.27	4.50	–	–	–	–	–	–	0.84	–
β-[$Me_2SnGalpa$] 24%	4.59	3.48	3.70	4.21	4.17	–	–	–	–	–	–	0.84	–
α-[$Me_2SnGalfa$] 12%	5.27	4.06	4.28	4.06	4.32	–	–	–	–	–	–	0.84	–
β-[$Me_2SnGalfa$] 49%	5.24	3.99	4.28	4.40	4.35	–	–	–	–	–	–	0.84	–
β-[n-$Bu_2SnGalfa$]	4.84	3.66	3.97	3.98	4.03	6.03	5.24	5.02	1.20	1.53	1.28	0.84	–
β-[$Ph_2SnGalfa$][b]	4.72	3.70	4.04	4.15[b]	4.19[b]	6.02	5.21	5.12	–	–	–	–	7.43 7.67
	H-1	H-2	H-3	H-4	H-5	OH-1	OH-2	OH-3	αCH$_2$	βCH$_2$	γCH$_2$	CH$_3$	Ph
α-[$Me_3SnGalpa$] 23%	5.30	3.83	3.91	4.30	4.46	–	–	–	–	–	–	0.83	–
β-[$Me_3SnGalpa$] 22%	4.58	3.50	3.69	4.22	4.10	–	–	–	–	–	–	0.83	–
α-[$Me_3SnGalfa$] 14%	5.27	4.07	4.28	4.07	4.32	–	–	–	–	–	–	0.83	–
β-[$Me_3SnGalfa$] 41%	5.24	3.99	4.29	4.41	4.35	–	–	–	–	–	–	0.83	–
β-[n-$Bu_3SnGalfa$] 53%	4.82	3.59	3.85	3.96	3.77	6.09	5.11	5.08	1.05	1.55	1.29	0.85	–

[a] Gal*p*a = *p*yranosidic ring;Gal*f*a = *f*uranosidic ring.
[b] For β-[$Ph_2SnGalfa$], H-4 and H-5 signals have been reassigned according to (^{1}H−^{119}Sn)-gHMBC spectrum (See Fig. 2).

Table 3
δ(^{13}C) values (ppm) of all the isomeric/anomeric forms of $R_3SnGala$ [R = Me (**4**), n-Bu (**5**)] compounds. The spectra were acquired in D_2O and DMSO-d_6 for **4** and **5**, respectively.

Compound[a]	C-1	C-2	C-3	C-4	C-5	C-6	αCH$_2$	βCH$_2$	γCH$_2$	CH$_3$
α-[$Me_3SnGalpa$] 23%	92.0	67.9	69.1	70.7	71.1		–	–	–	3.83
β-[$Me_3SnGalpa$] 22%	95.8	71.4	72.7	70.1	75.2		–	–	–	3.83
β-[$Me_3SnGalfa$] 14%	95.3	75.5	73.6	82.8	n.d.		–	–	–	3.83
β-[$Me_3SnGalfa$] 41%	101.7	80.2	75.6	85.7	71.8		–	–	–	3.83
α-[n-$Bu_3SnGalfa$] 53%	101.1	81.7	75.2	82.2	69.4	175.9	19.1	28.2	27.1	14.0

[a] Gal*p*a = *p*yranosidic ring; Gal*f*a = *f*uranosidic ring.

2.3.3. Measurement of phosphatidylserine exposure

The externalization of phosphatidylserine (PS) to the cell surface was detected by flow cytometry by double staining with annexin V-fluorescein isothiocyanate (annexin V-FITC)/propidium iodide (PI). Phosphatidylserine, which is normally located on the cytoplasmic surface of cell membranes, is exposed on the cell surface upon induction of apoptosis. Annexin V binds to phosphatidylserine and is used to identify the earliest stage of apoptosis. PI, which does not enter cells with intact membranes, is used to distinguish between early apoptotic cells (annexin V-FITC positive and PI negative) and late apoptotic cells (annexin V-FITC/PI-double positive).

MCF-7 and HCT-116 cells were seeded in triplicate in 24-wells culture plates at a density of 5.0×10^4 cells/cm^2. After overnight incubation, the cells were washed with fresh medium and incubated with the compounds in RPMI. After 24 h, cells were harvested by trypsinization and adjusted at 1.0×10^6 cells/mL with combining buffer according to the manufacturer's instructions (eBioscience, San Diego, CA). An aliquot (100 µL) of cell suspended solution was added to a new tube, and incubated with Annexin V-FITC and PI solution according to the manufacturer's instructions (eBioscience, San Diego, CA) at room temperature in the dark for 15 min. Then samples of at least 1.0×10^4 cells were analyzed by fluorescence-activated cell sorting (FACS) analysis by Epics XL™ flow cytometer using Expo32 software (Beckman Coulter, Fullerton, CA), using appropriate 2-bidimensional gating method.

2.3.4. Measurement of mitochondrial transmembrane potential

Mitochondrial transmembrane potential (Δψm) was assayed by flow cytofluorometry, using the cationic lipophilic dye 3,30-dihexyloxacarbocyanine iodide [DiOC6(3)] (Molecular Probes, Inc.) which accumulates in the mitochondrial matrix.

Changes in mitochondrial membrane potential are indicated by a reduction in the DiOC6(3) concentration, for 15 min at 37 °C. After centrifugation, cells were washed with PBS (Phosphate-Buffered Saline) and suspended in 500 µL PBS. Fluorescence intensities were analyzed in at least 1×10^4 cells for each sample.

2.3.5. Cell cycle analysis

Cell cycle stage was analyzed by flow cytometry. Aliquots of 1×10^6 cells were harvested by centrifugation, washed with PBS and incubated in the dark in a PBS solution containing 20 µg/mL PI and 200 µg/mL RNase, for 30 min, at room temperature. Then, samples were immediately subjected to FACS as above detailed. At least 1×10^4 cells were analyzed for each sample.

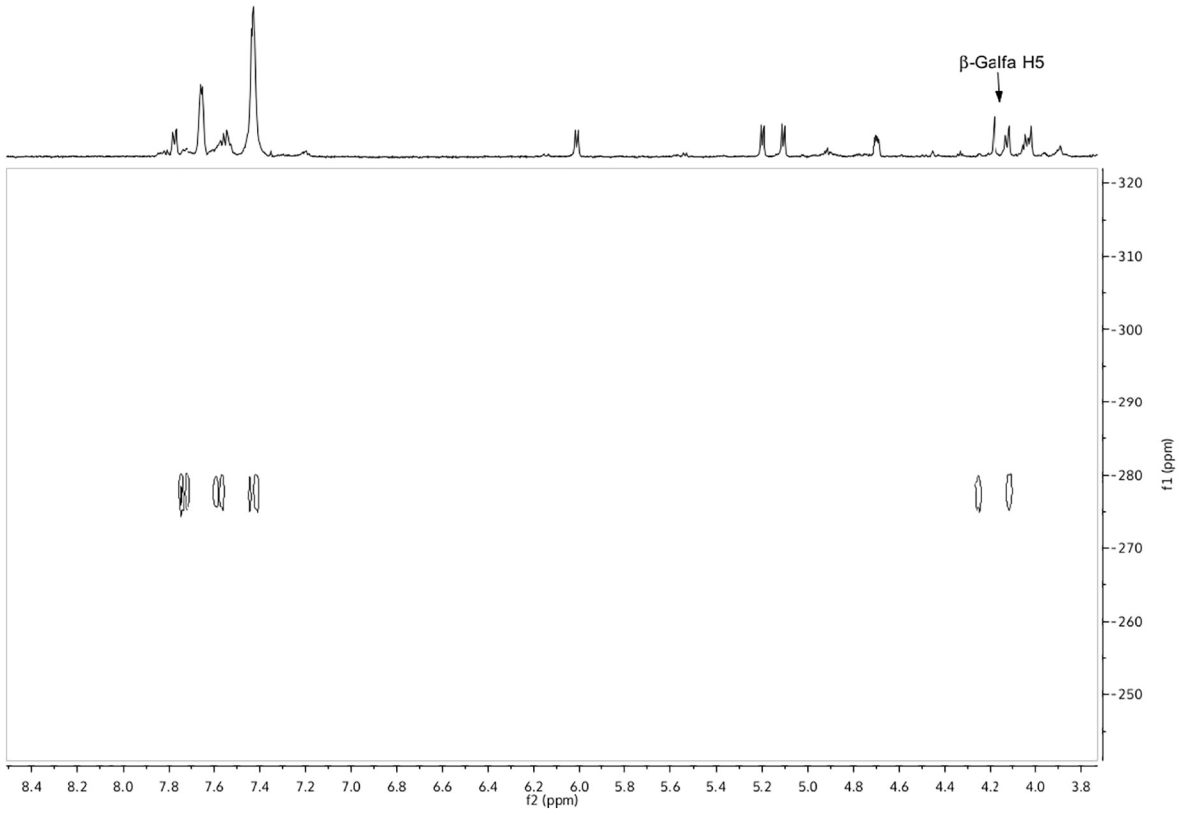

Fig. 2. (^{1}H—^{119}Sn)-gHMBC spectrum of **3** in DMSO-d_6. ^{119}Sn—^{1}H5 bond-connection present in the β-furanosidic form is shown.

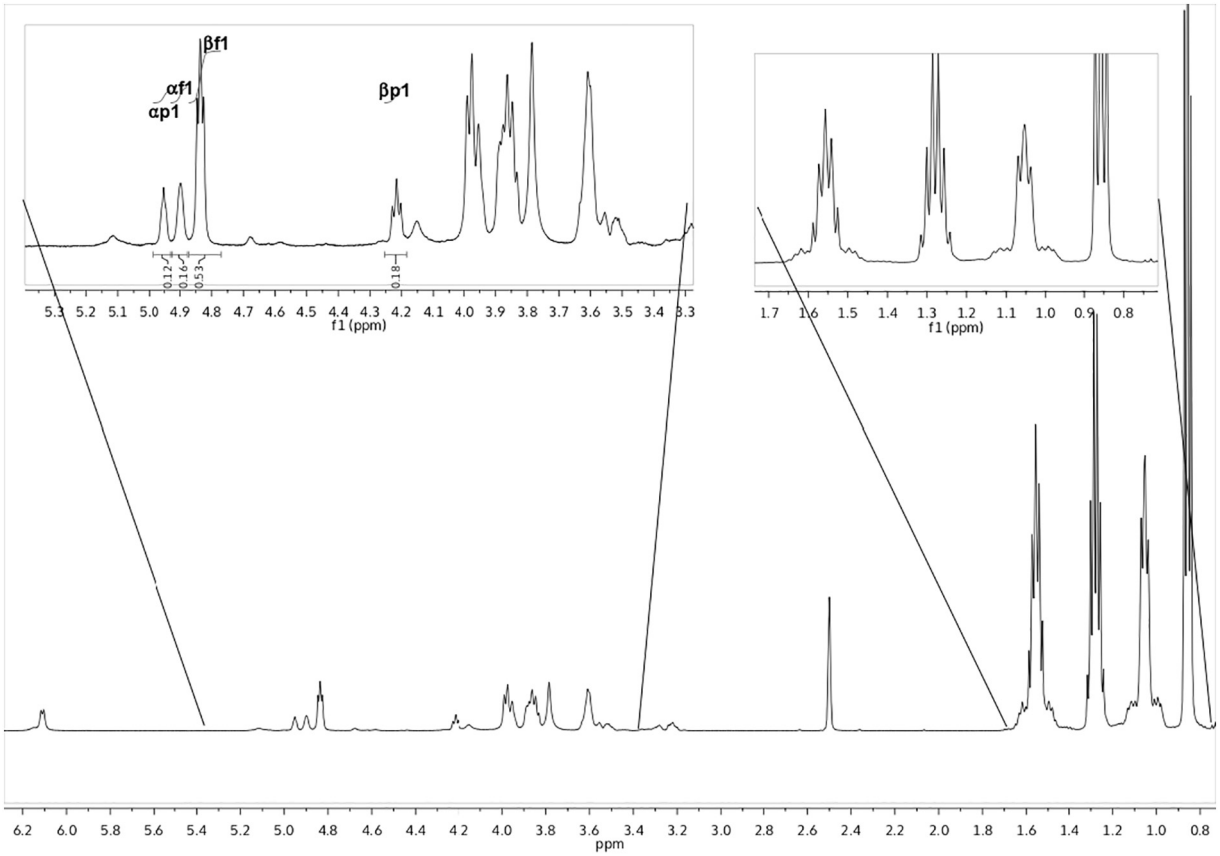

Fig. 3. Presaturated ^{1}H NMR spectrum of **5** in DMSO-d_6 and panels zoom of (*top left*) proton signals of the ligand (the OH1 signal at 6.09 ppm is not included in this panel), and (*top right*) proton signals of the butylic chains.

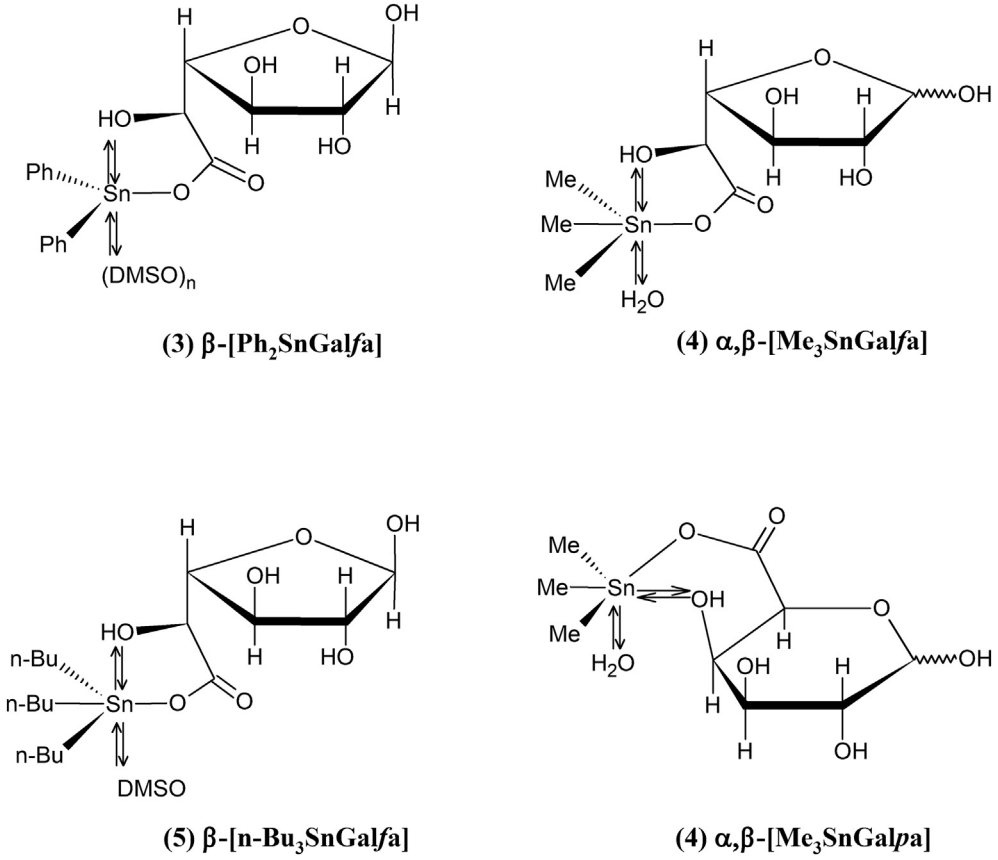

Fig. 4. Schematic solution configurations proposed for **3**, **4**, and **5**. Interaction with the appropriate solvent molecules is also reported. For compound **3**, n = 1, 2. For compound **4**, both pyranosidic and furanosidic observed forms were given. Exchanging sites are indicated with double arrows.

2.3.6. Interaction with DNA. Melting experiments

Potential interactions between Sn-compounds and calf thymus DNA were investigated by dissolving CT-DNA at the concentration 0.14 mM in nucleotides, using the value of ε_{260} = 6600 $cm^{-1}\,M^{-1}$ [50]. The DNA was dissolved in 2700 µL of an aqueous solution 100 mM in NaCl and 10 mM in sodium cacodylate at pH 7.0. Each experiment was conducted at two different Sn/P ratio: a low ratio corresponding to 1 Sn each 20 P (*i.e.* one Sn per helix turn) and a higher ratio corresponding to 1 Sn per base-pair. The Sn derivatives were dissolved in DMSO. The required amount of Sn compound (2-20 µL) was added to the dissolved CT-DNA, and a compensating volume of DMSO was added to the low ratio sample and to the pure CT-DNA cuvette used as reference. After an equilibrating time of 30 min, the denaturation profile of the two samples and reference were recorded on a Cary 100 spectrophotometer at 260 nm, from 20 °C to 90 °C with a heating gradient of 0.4 °C/min.

3. Results and discussion

3.1. Infrared spectra

Infrared absorptions of compounds **1-3**, are given as Supplementary Material (Table S1). For these compounds, the observed bands assigned to νOH, ν_{as}COO, ν_sCOO and ν(Sn−C) are in very good agreement with literature [20]. For HGala·H_2O and the newly synthesized **4** and **5** compounds, the relevant infrared frequencies are given in Table 1.

The ν(COOH) of HGala, showed a red-shift, analogously to R_2SnGala compounds [20], indicating deprotonation and ensuing coordination of the carboxylic group to the R_3Sn(IV) moieties. Moreover, the high $\Delta\nu$ = [$\nu_{as}(COO^-)$-$\nu_s(COO^-)$] values of the coordinated $COO^{(-)}$, are in agreement with an ester-type coordination. The ν(OH) also showed a red-shift, pointing to a breaking and/or rearrangements of the hydrogen interactions network due to coordination.

Bands of medium intensity have been assigned to ν_{as}(Sn−C) and ν_s(Sn−C) stretching at 594 and 530 cm^{-1} for compound **4** and at 610 and 542 cm^{-1} for compound **5**.

3.2. NMR in solution

The δ(^{1}H) values of all the compounds, and the δ(^{13}C) values only for **4** and **5** are given, respectively, in Tables 2 and 3.

3.2.1. ^{1}H and ^{13}C NMR

^{1}H and ^{13}C spectra for the already presented R_2SnGala compounds are very similar to the previously reported data [20]. For **1**, small discrepancies in $\delta(^1H)$ and composition of the isomeric mixture, with respect to ref. [20], are most likely due to the different pD conditions (pD = 7 [20] *vs.* pD = 5.1 in this work, obtained at the working temperature as: pD = pH + 0.41 [51]). The measured $^2J(^{119}Sn, ^1H)$ = 88 Hz satellites, flanking the methyl signal, allowed to estimate [52] a θ(C-Sn-C) of *ca.* 141°, also in very good agreement with the previous report [20]. Moreover, for **3**, analysis of the (^{1}H−^{119}Sn)-gHMBC spectrum (Fig. 2) allowed to reassign [20] the resonances of H4 and H5, by interchanging the corresponding values. For the newly synthesized **4**, as for **1**, a mixture of the four isomers was observed and, also in this case, the Me_3Sn(IV) moiety enhances the amount of the coordinated furanosidic form of the ligand, with percentages very close to those observed for **1** [20]. Moreover, the $^2J(^{119}Sn, ^1H)$ value of 86 Hz, measured from the satellites in the ^{1}H spectrum, allowed to calculate a θ(C-Sn-C) value of *ca.* 139° [52]. This value points to a skew-octahedral local geometry at the tin center, due either to the coordination with the carboxylate group and to the occurrence of solvent molecules and/or OH groups of the ligand, in the tin sphere of

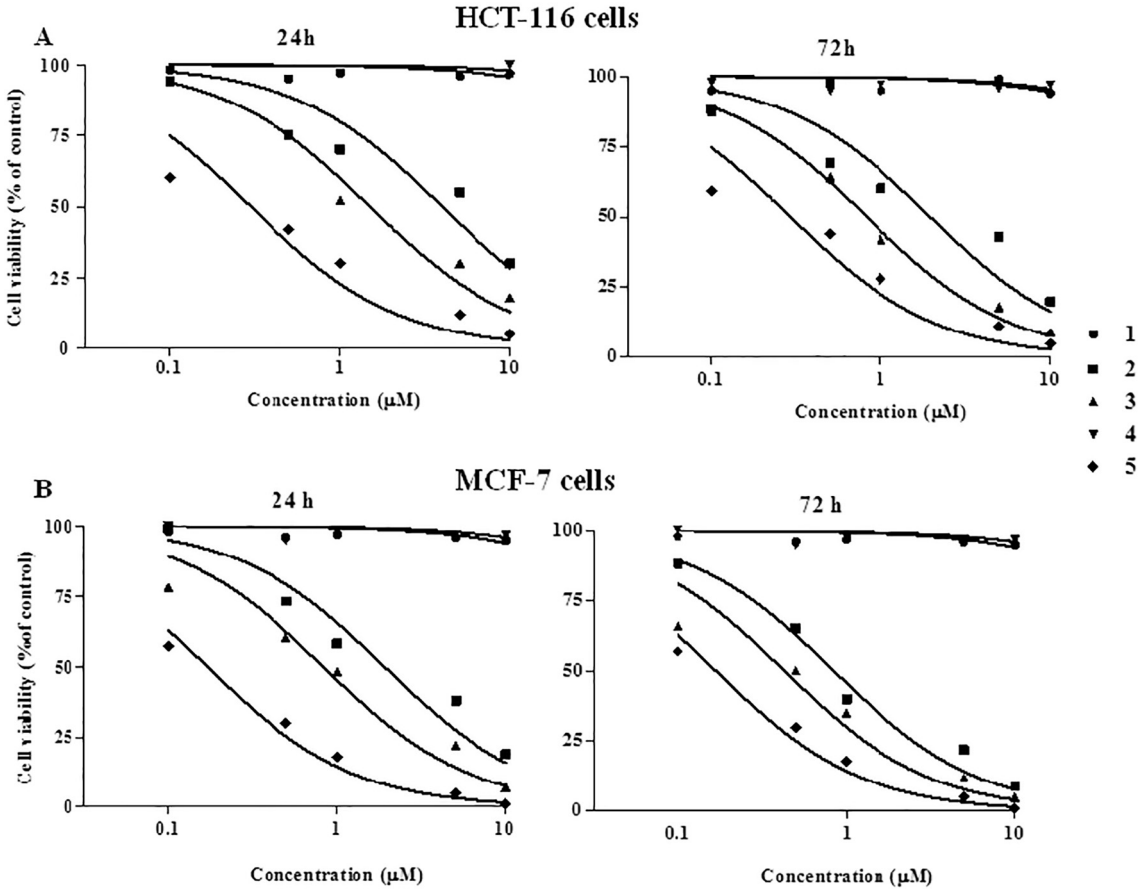

Fig. 5. Effect of **1**-**5** on the viability of HCT-116 (**A**) or MCF-7 (**B**) cells after 24 h or 72 h treatment. Cells were treated with the compounds and cell survival was measured by MTT assay in comparison to cells treated with vehicle alone (control), as reported in the *Experimental* section. Values are the mean ± SD of three separate experiments carried out in triplicate.

Table 4
Calculated IC_{50} values[a] (μM) of active **2**,**3**, and **5** compounds at different incubation times.

Compound	IC_{50} ± SD			
	HCT-116		MCF-7	
	24 h	72 h	24 h	72 h
2	3.94 ± 0.26	1.97 ± 0.12[b]	1.89 ± 0.15	0.84 ± 0.06[b]
3	1.48 ± 0.13	0.82 ± 0.06[b]	0.83 ± 0.06	0.43 ± 0.03[b]
5	0.29 ± 0.02	0.28 ± 0.03	0.16 ± 0.01	0.17 ± 0.02
Cisplatin	40.21 ± 2.07	nd	16.45 ± 1.11	nd

[a] Values are the mean ± SD of three separate experiments in triplicate.
[b] Significantly different ($p < 0.05$) from the relevant value calculated at 24 h (Student's *t*-test). nd, not determined.

coordination [20–22]. The ^{1}H spectrum of **5** (Fig. 3), showed all the four isomeric forms of the compound, at variance to what previously observed for **2** [20]; also in this case the β-furanosidic form was the preferred one. In this context, due to the relatively low solubility of **5** a complete assignment of all the species in solution was not possible; thus, we report only ^{1}H and ^{13}C data for the predominant isomeric form (the relevant 1D $^{13}C\{^{1}H\}$ and 2D [^{1}H,^{13}C]-gHSQCAD spectra are given in Figs. S1 and S2 as Supplementary Material).

^{13}C NMR resonances of **4** and **5** are very similar to the analogous $R_2SnGala$ compounds [20]. For **4**, a $^{1}J(^{13}C,^{1}H)$ value of 718 Hz was obtained from the satellites in the ($^{1}H-^{119}Sn$)-HSQC spectrum, from which a θ(C-Sn-C) value of *ca.* 140° was estimated [52], in very good agreement with the 139° value obtained from the corresponding ^{2}J (^{119}Sn, ^{1}H) satellites. For **5**, a $^{1}J(^{13}C,^{1}H)$ value of *ca.* 460 Hz was obtained from the satellites in the ($^{1}H-^{119}Sn$)-HSQC spectrum, corresponding to a θ(C-Sn-C) of *ca.* 120 ± 1° [53] that points to a local trigonal-bipyramidal geometry around tin, where the fifth coordination site could be involved in a competitive exchange between a suitable OH group and/or a solvent molecule [20–22,54].

3.2.2. *^{119}Sn NMR*

For **1** and **2**, ^{119}Sn spectra showed a single peak at −127 ppm and − 126 ppm, respectively, in good agreement with the −131 ppm and − 127 ppm values previously reported [20].

For **3**, $\delta(^{1}H)$ and $\delta(^{13}C)$ have been firstly reported elsewhere [20], while $\delta(^{119}Sn)$ was not observed previously due to the low solubility of **3** in DMSO-d_6. However, exploitation of the ($^{1}H-^{119}Sn$)-gHMBC technique, has now allowed to detect the ^{119}Sn resonance at −277 ppm. This value allows to infer a local coordination environment around the tin atom, at the boundary between penta- and hexa-coordinated tin. This is in agreement with the chelating behavior of the ligand, and with the occurrence of solvent molecule(s) in the tin sphere, as observed for other "hard" metal complexes in solution and in the solid state [55–57].

For **4**, a ^{119}Sn peak was observed at −100 ppm (LW ≈ 300 Hz). The $\delta(^{119}Sn)$ is in accord with a penta-coordinated tin, even if the 141° value of θ(C-Sn-C), estimated from the relevant $^{2}J(^{119}Sn, ^{1}H)$ satellites, is in better agreement for a skew-octahedral geometry. This discrepancy is resolved by considering the LW value, that indicates that tin undergoes chemical exchange due to isomeric interconversion together with, conceivably, exchange processes involving solvent molecules and/or OH groups. For **5**, a peak at −19.7 ppm (LW of *ca.* 130 Hz) has been observed, together with a less intense resonance at −16.5 ppm (LW *ca.*

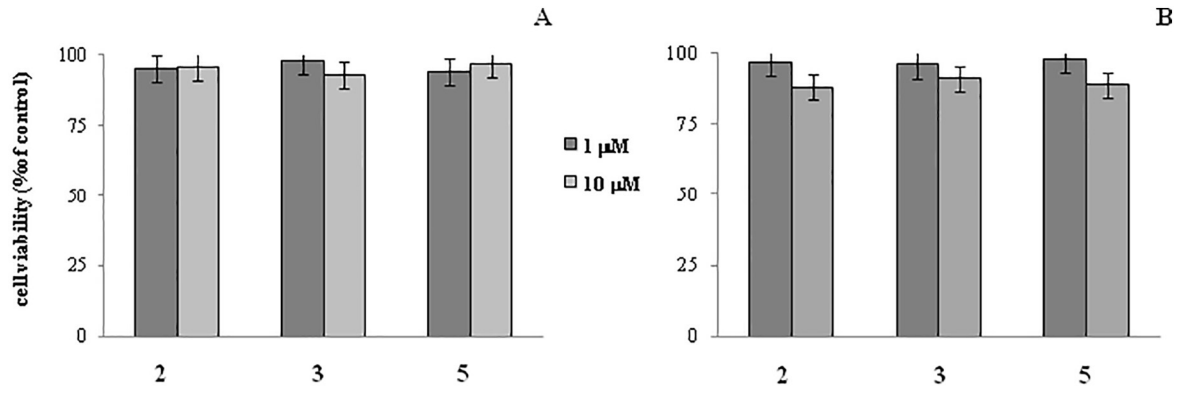

Fig. 6. Effect of **2**, **3**, and **5** on the viability of intestinal normal-like differentiated Caco-2 cells (**A**) and Chang liver (**B**). 15-days post-confluence monolayers of Caco-2 and Chang liver cells were incubated for 24 h in the absence (control) or in the presence of the compounds at the indicated concentrations and cell viability was assessed by MTT test as reported in the *Experimental* section. Values are the mean ± SD of two separate experiments carried out in triplicate.

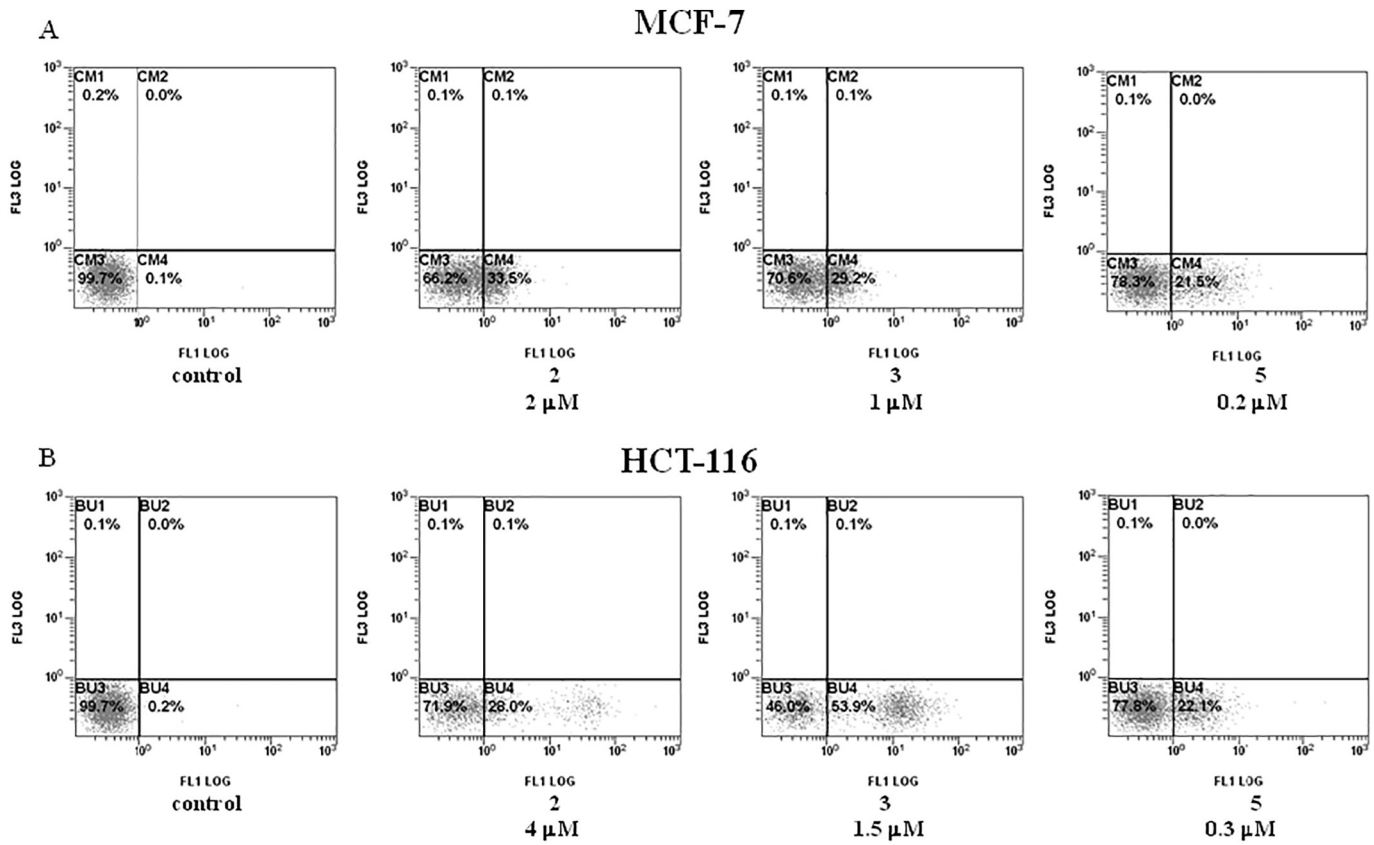

Fig. 7. Flow cytometric analysis for the quantification, by AnnexinV/PI double staining, of **2**, **3**, and **5**- induced apoptosis in MCF-7 (**A**) and HCT-116 (**B**) cells. Cell monolayers were incubated for 24 h in the absence (control) or in the presence of individual compounds and submitted to double staining with Annexin V/PI as reported in *Experimental*. CM3 or BU3, viable cells (AnnexinV-/PI-); CM4 or BU4, cells in early apoptosis (AnnexinV + /PI-); CM2 or BU2, cells in late apoptosis (AnnexinV + /PI +); CM1 or BU1, necrotic cells (AnnexinV-/PI +). Representative images of three experiments with comparable results.

120 Hz) (Supplementary Material, Fig. S3). The two peaks correspond to the two pairs of exchanging cyclic isomers, and the furanosidic ones correspond to the more intense resonance. The $\delta(^{119}Sn)$ values for **5**, lie at the boundary between tetra- and penta-coordinated butyltin(IV) derivatives. Taking into account the value of *ca.* 120 ± 1°, calculated for θ(C-Sn-C) from $^{1}J(^{13}C,^{1}H)$ satellites, these findings might be considered in agreement with the occurrence of the anomeric/isomeric interconversion and solvent exchange processes involving tin nucleus.

In Fig. 4, a schematic depiction of the presumed structures in solution for **3**, **4**, and **5** are given (structures for **1** and **2** have been already proposed elsewhere [20,23]).

3.3. Anti-cancer study

Anti-cancer properties of **1-5** were evaluated against human tumor cell lines of intestinal carcinoma (HCT-116 cells) and breast adenocarcinoma (MCF-7 cells). Monolayer cultures treated for 24 h or 72 h with 0.1–10 µM concentrations of the compounds, were examined by MTT assay for the cell viability. While **1** and **4** did not affect the cell growth at any of the considered concentrations or incubation times, **2**, **3** and **5** inhibited the viability of either HCT-116 or MCF-7 cells in dose-dependent manner (Fig. 5). On the basis of the IC_{50} values calculated at 24 h incubation, cytotoxicity of the compounds followed the order **5** > **3** > **2** and appeared much higher than that evaluated for

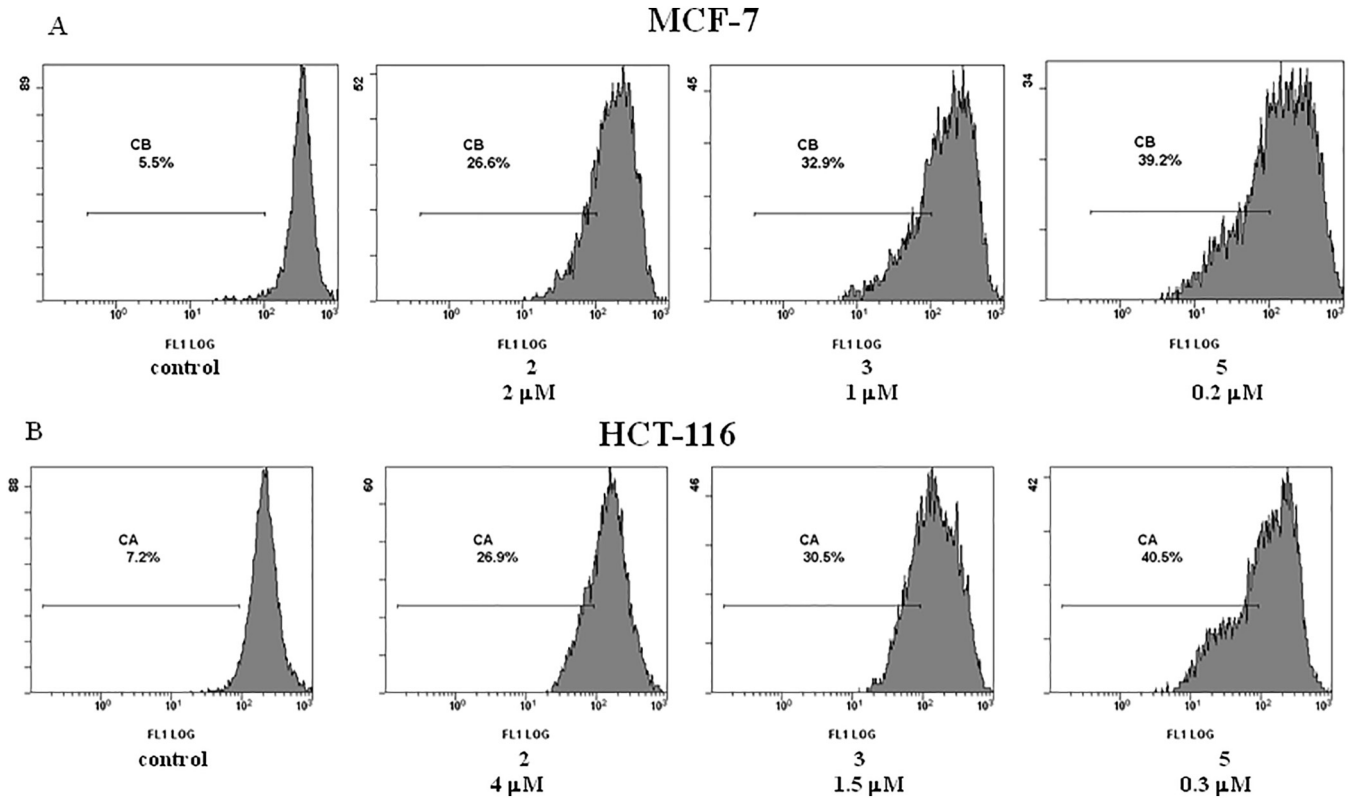

Fig. 8. Effects of **2**, **3**, and **5** on dissipation of mitochondrial transmembrane potential (Δψm) in MCF-7 (**A**) and HCT-116 (**B**) cells. After treatment with the compounds for 24 h, cells were stained with the lipophilic cationic fluorochrome DiOC6(3) and flow cytometry analysis was carried out as reported in Methods. Representative images of three experiments with comparable results.

cisplatin, used for comparison in the same experimental conditions (Table 4). Our findings are in agreement with the knowledge that diorganotin(IV) compounds exhibit lower activity than triorganotin(IV) ones [7]. Moreover, while cell growth inhibition by **2** and **3** increased with the exposure time, as shown by lower IC_{50} values measured at 72 h, the effect on cell survival of **5** appeared time-independent (Fig. 5 and Table 4).

In order to determine the selectivity of the *in vitro* cytotoxicity of the active $R_nSnGala$ (n = 2,3) compounds, some additional experiments were conducted on intestinal normal-like differentiated Caco-2 cells and Chang cells as normal hepatocyte model. As shown in Fig. 6, at the concentrations effective to inhibit the growth of HCT-116 and MCF-7 tumor cells, the compounds did not affect to a large extent the viability of both normal-like cells. Although selectivity for cancer cells cannot be easily derived from comparison of toxicity parameters in different cell cultures, these data indicated that the active **2**,**3** and **5** compounds show preferential toxicity towards cancer cells.

The effects of the compounds on the occurrence of apoptosis or cell death were examined by FACS analysis of Annexin V- and PI-stained either HCT-116 or MCF-7 cells. The selected concentrations are the IC_{50} values measured at 24 h for each cell line. Flow cytometric analysis showed that, after 24 h of treatment, the percentage of total apoptotic population was significantly increased in both the cancer cell lines compared to untreated control, whatever the compound was (Fig. 7).

More precisely, **2** treatment caused an increase of early apoptotic cells of the 33.5% (MCF-7) and 28% (HCT-116), **3** of the 29.2% (MCF-7) and 53.9% (HCT-116) and **5** of the 21.5% (MCF-7) and 22.1% (HCT-116).

The mitochondrion plays a key role in the apoptotic mechanism of cell death and loss of transmembrane mitochondrial potential (Δψm) is a reliable marker of intrinsic apoptosis pathway. Measurements of Δψm using the lipophilic cationic fluorochrome DiOC6(3) and flow cytometry analysis, showed that the compounds induced, in both MCF-7 and HCT-116 cells, a significant decrease in DiOC6(3) uptake, indicating induction of mitochondrial dysfunction (Fig. 8).

Effects of the three active **2**, **3**, and **5** compounds on either MCF-7 or HCT-116 cell cycle distribution was determined by flow cytometric analysis after staining of DNA with PI. After 24 h of treatment, compounds **2** and **3** induced a marked accumulation of cells in the subG0/G1 phase of cell cycle, which is representative of cells with fragmented DNA, with a concomitant increase of the percentage of cell population in the G0/G1 phase, in both the cell lines (Fig. 9). On the contrary, although 24 h treatment with compound **5** causes an obvious appearance of cells in sub-G1 as compared to untreated control, we failed to detect any significant perturbation of cell cycle phases, confirming that the compound does not own anti-proliferative properties.

3.3.1. *Uptake study of compound* **5**

In order to explain the peculiar behavior of compound **5**, we have studied its chemical stability in many DMSO-d_6/D_2O solutions of different compositions.

Going from the prevalent DMSO-d_6 to the prevalent D_2O mixtures, the trend of the observed signals pointed only to a solvent effect, characterized by: i) a slight deshielding of the $\delta(^{119}Sn)$, as a result of the (partial) displacement of DMSO-d_6 by D_2O in the tin coordination sphere, and ii) a broadening of the $\delta(^{119}Sn)$ in the prevalent D_2O mixtures due to the different anomerization kinetics as already observed in DMSO-d_6 and D_2O [23]. This allowed to discard, at the NMR experimental conditions, the occurrence of any appreciable decomposition of **5** to yield hydrolysis products (details and selected ^1H and ^{119}Sn spectra are given as Supplementary Material). Indeed, at variance with the NMR experiment, in the cell culture medium: i) water was highly predominant with respect to DMSO (0.1%) and ii) the concentrations of the compound (*ca.* 0.1 to 10 μM) was much lower than

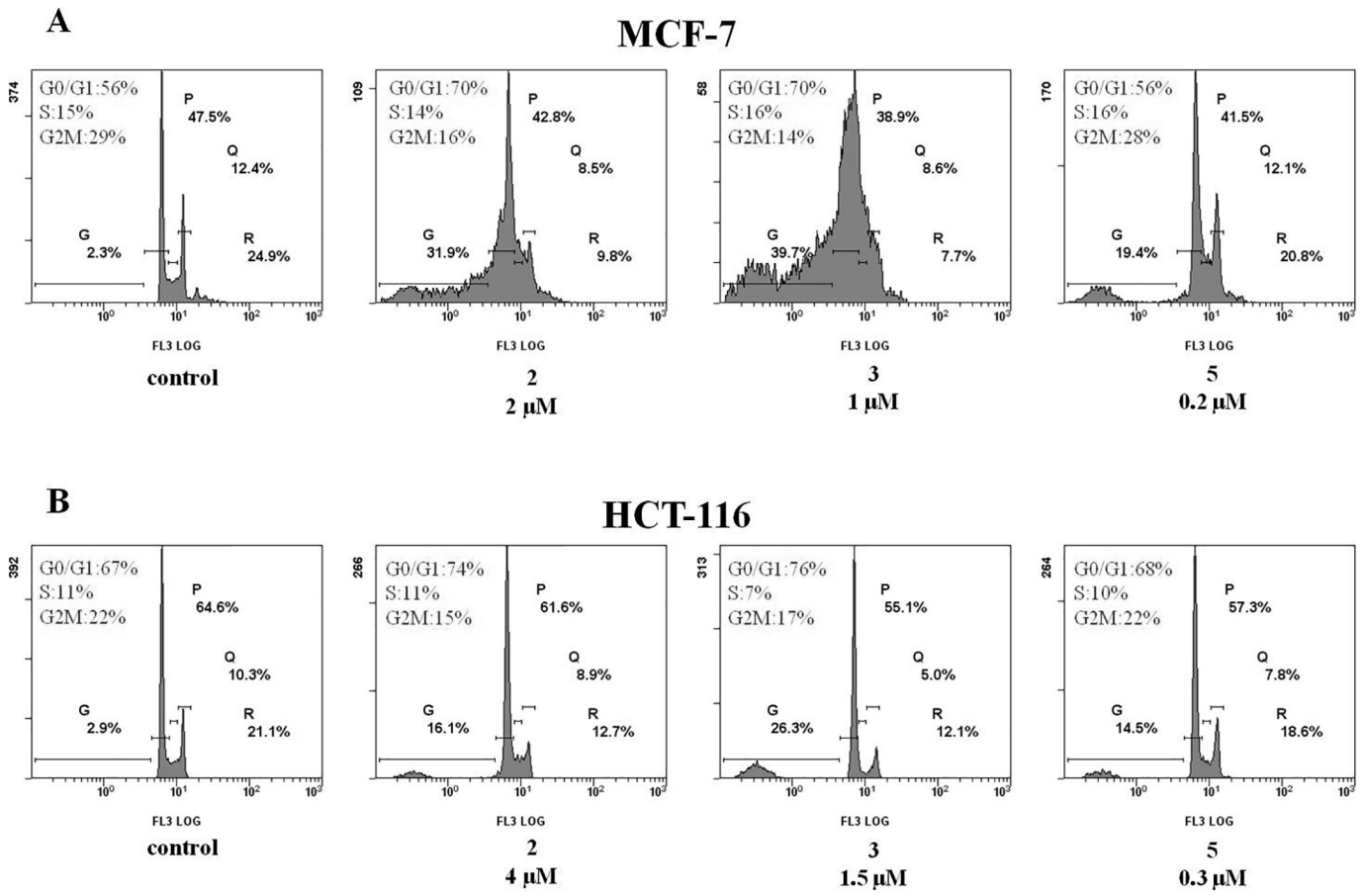

Fig. 9. Effect of **2**, **3**, and **5** on cell cycle distribution of MCF-7 (**A**) or HCT-116 (**B**) cells. Flow cytometric analysis of propidium iodide-stained cells after 24 h treatment with the compounds. The percentage of cells in the different phases of the cycle was calculated by Expo32 software. Percentage of viable cells in the different phases are given in each picture. Representative images of three experiments with comparable results.

Table 5
Amount of Sn (µg), measured by ICP spectrometer, for HCT-116 and MCF-7 cell lines at different times of treatment for compound **5**. Results are given with uncertainty of ± 0.001 µg. The results are referred to a theoretical tin total content of 0.0235 µg.

Cell line	HCT-116						MCF-7			
Sample	Cells			Medium			Cells		Medium	
Incubation time	6 h	24 h	72 h	6 h	24 h	72 h	24 h	72 h	24 h	72 h
	0.002	0.002	0.001	0.026	0.022	0.025	0.000	0.003	0.026	0.022

that used to acquire NMR spectra. However, the loss of cytotoxic activity of **5** after 24 h, led to suppose that the tributyltin(IV) moiety could experience a metabolic degradation (*vide infra)*.

Thus, we also checked the presence, and the relevant amount, of tin metal in cells treated with **5**, by ICP measures on both cell lines. In particular, for each cell line we measured the residual amount of Sn, after 24 and 72 h, both in medium and in cells. The results are presented in Table 5.

Data in Table 5 indicate that both after 24 h (when it shows antiproliferative activity) and 72 h (when its antiproliferative activity is inhibited), compound **5** is not localized into the cells and then it seems to be unable to cross cell membrane. For HCT-116 cells lines, we also performed a further uptake study after 6 h of treatment obtaining quite similar results (Table 5). Although it has been reported that organotin (IV) compounds can penetrate into the cells of the HCT-116 line [58], it is possible that **5** acts by means of cation-cell membrane interaction. Our findings could also imply the activation of an inhibiting (detoxication) mechanism for the cells towards this compound.

3.3.2. Interaction with DNA

Interaction with DNA may be one of the potential pathways of toxicity of organotin(IV) derivatives [9,10]. In this context, we explored also the possibility of interaction between the compounds and calf-thymus DNA, at the Sn/P ratios 1/20 and 1/10 in 0.1 M NaCl solutions at pH 7.0.

No significant differences were found in the melting points, identified by the first derivative method, nor appreciable differences were detected by superimposition of the double normalized profiles. Thus, all the melting experiments failed to indicate a difference between the denaturing profile of the Sn-DNA samples and that of DNA alone. Only for compound **5**, the lack of interaction with CT-DNA was further checked by a circular dichroism experiment performed adding to a CT-DNA solution successive portions of **5** solution to have the Sn/phosphate ratios increasing from 0 to the high ratio (100%) (results of the experiment are given in Supplementary Material, Fig. S7). All findings ultimately testify the lack of any involvement of DNA in the cytotoxic mechanism of the organotin(IV) compounds here studied.

4. Conclusions

We compared the anti-tumor activity of di-(**1-3**) and tri-organotin (IV) (**4**,**5**) compounds with D-(+)-Galacturonic acid upon two cell lines of human epithelial tumor, namely intestinal carcinoma HCT-116 cells and breast adenocarcinoma MCF-7 cells. The two novel compounds **4** and **5** were characterized by FT-IR and ^{1}H, ^{13}C, and ^{119}Sn NMR spectroscopy, while for the already synthesized compound **3** a new assignment of H4 and H5, as well as the first observation of the ^{119}Sn NMR resonance were reported here.

The biological investigation showed anti-cancer activity for compounds **2**, **3**, and **5** with an activity scale according to: **5** > **3** > **2**, while **1** and **4** were ineffective on either cell lines.

Interestingly, none of the compounds investigated affected the viability of normal intestinal or liver cells, indicating selectivity towards tumor cells. Cytotoxic activity of the active compounds was in the micro-submicromolar range and **5** showed a cell growth-inhibitory potency two orders of magnitude higher than cisplatin, the most clinically established chemotherapeutic drug. The cell death of MCF-7 and HCT-116 induced by the compounds was found to be apoptotic by measuring the exposure of phosphatidylserine to the outer membrane and the loss of mitochondrial potential. Compounds **2** and **3** inhibited the cell growth in a time-dependent manner and their anti-proliferative mechanism was G0/G1-phase arrest. This finding is consistent with the shown inability of the compounds to bind DNA, since interaction of drugs with DNA leads to induction of S-G2/M arrest.

The activity of **5** resulted in time-independent cytotoxic effects. In this context, ICP measurements confirmed that Sn is quantitatively absent in the cell lines after 6 h, 24 h or 72 h of treatment with **5**, suggesting compound's inability to cross cell membrane. Thus, degradation, or metabolization, of **5** by cells cannot be excluded. Additional proofs of the most probable mechanisms here discussed deserve to be collected and investigations are in progress in our laboratories. In any case, repeated administration of the very active compound **5** could be envisaged for potential biomedical applications of the metallodrug. The compounds studied are proposed as promising organometallic-based drugs.

Conflict of interest

The authors declare that they have no conflicts of interest with the contents of this article.

Acknowledgments

NMR spectra acquired with the Bruker Avance II DMX spectrometer, were provided by Centro Grandi Apparecchiature – ATeNCenter – Università di Palermo, Italy, funded by P.O.R. Sicilia 2000–2006, Misura 3.15 Quota Regionale.

Appendix A. Supplementary data

Supplementary data to this article can be found online at https://doi.org/10.1016/j.jinorgbio.2018.04.006.

References

[1] A.-M. Florea, D. Büsselberg, Cancers 3 (2011) 1351–1371.
[2] T. Storr, K.H. Thompson, C. Orvig, Chem. Soc. Rev. 35 (2006) 534–544.
[3] S.M. Cohen, Curr. Opin. Chem. Biol. 11 (2007) 115–120.
[4] P.C. Bruijnincx, P.J. Sadler, Curr. Opin. Chem. Biol. 12 (2008) 197–206.
[5] S.H. van Rijt, P.J. Sadler, Drug Discov. Today 14 (2009) 1089–1097.
[6] A. Alama, B. Tasso, F. Novelli, F. Sparatore, Drug Discov. Today 14 (2009) 500–508.
[7] S.K. Hadjikakou, N. Hadjiliadis, Coord. Chem. Rev. 253 (2009) 235–249.
[8] D. Gaynor, D.M. Griffith, Dalton Trans. 41 (2012) 13239–13257.
[9] S. Tabassum, C. Pettinari, J. Organomet. Chem. 691 (2006) 1761–1766.
[10] Ž. Jakšic, A. Pagliarani, F. Trombetti, V. Ventrella (Eds.), Biochemical and Biological Effects of Organotins, Mechanisms of Organotin Induced Apoptosis, Bentham Science Publishers Ltd, 2012, pp. 149–163.
[11] L. Pellerito, L. Nagy, Coord. Chem. Rev. 224 (2002) 111–150.
[12] A.K. Saxena, F. Huber, Coord. Chem. Rev. 95 (1989) 109–123.
[13] M. Gielen, Coord. Chem. Rev. 151 (1996) 41–51.
[14] R.A. Dwek, Chem. Rev. 96 (1996) 683–720.
[15] T. Angata, A. Varki, Chem. Rev. 102 (2002) 439–470.
[16] S. Tabassum, S. Yadav, F. Arjmand, Inorg. Chim. Acta 423 (Part B) (2014) 38–45.
[17] M. Tanaka, H. Kataoka, M. Mabuchi, S. Sakuma, S. Takahashi, R. Tujii, H. Akashi, H. Ohi, S. Yano, A. Morita, T. Joh, Anticancer Res. 31 (2011) 763–769.
[18] S. Hirohara, M. Obata, H. Alitomo, K. Sharyo, T. Ando, M. Tanihara, S. Yano, J. Photochem. Photobiol. B 97 (2009) 22–33.
[19] A. Szorcsik, L. Nagy, B. Gyurcsik, G. Vankó, R. Krämer, A. Vértes, T. Yamaguchi, K. Yoshida, J. Radioanal. Nucl. Chem. 260 (2004) 459–469.
[20] N. Bertazzi, G. Bruschetta, G. Casella, L. Pellerito, E. Rotondo, M. Scopelliti, Appl. Organomet. Chem. 17 (2003) 932–939.
[21] A. Bagno, N. Bertazzi, G. Casella, L. Pellerito, G. Saielli, I.D. Sciacca, J. Phys. Org. Chem. 19 (2006) 874–883.
[22] N. Bertazzi, G. Casella, F. Ferrante, L. Pellerito, A. Rotondo, E. Rotondo, Dalton Trans. (2007) 1440–1446.
[23] A. Rotondo, E. Rotondo, G.A. Casella, G. Grasso, Dalton Trans. (2008) 596–601.
[24] M. Nath, M. Vats, P. Roy, Inorg. Chim. Acta 423 (Part B) (2014) 70–82.
[25] R.A. Khan, S. Yadav, Z. Hussain, F. Arjmand, S. Tabassum, Dalton Trans. 43 (2014).
[26] M. Nath Mridula, J. Solut. Chem. 45 (2016) 445–462.
[27] A. Lakatos, R. Bertani, T. Kiss, A. Venzo, M. Casarin, F. Benetollo, P. Ganis, D. Favretto, Chem. Eur. J. 10 (2004) 1281–1290.
[28] F. Caruso, M. Bol-Schoenmakers, A.H. Penninks, J. Med. Chem. 36 (1993) 1168–1174.
[29] J. Alper, Science 291 (2001) 2338–2343.
[30] P.A. Markov, S.V. Popov, I.R. Nikitina, R.G. Ovodova, Y.S. Ovodov, Russ. J. Bioorg. Chem. 37 (2011) 817–821.
[31] C. Wei, P. He, L. He, X. Ye, J. Cheng, Y. Wang, W. Li, Y. Liu, Int. J. Biol. Macromol. 109 (2018) 65–75 (S).
[32] J.-H. Lee, Y.-K. Lee, Y.-R. Choi, J. Park, S.K. Jung, Y.H. Chang, Int. J. Biol. Macromol. 111 (2018) 311–318.
[33] S.-H. Hwang, M.-S. Shin, T.J. Yoon, K.-S. Shin, Int. J. Biol. Macromol. 107 (2018) 2695–2700.
[34] H.E. Guard, W.M. Coleman, M.M. Ross, Carbohydr. Res. 235 (1992) 41–51.
[35] M.A. Girasolo, A. Attanzio, P. Sabatino, L. Tesoriere, S. Rubino, G. Stocco, Inorg. Chim. Acta 423 (Part B) (2014) 168–176.
[36] M.A. Girasolo, L. Tesoriere, G. Casella, A. Attanzio, M.L. Capobianco, P. Sabatino, G. Barone, S. Rubino, R. Bonsignore, Inorg. Chim. Acta 456 (2017) 1–8.
[37] S.L. Patt, J.N. Shoolery, J. Magn. Reson. 46 (1982) 535–539.
[38] A. Bax, D.G. Davis, J. Magn. Reson. 63 (1985) 355–360.
[39] C. Griesinger, G. Otting, K. Wüthrich, R.R. Ernst, J. Am. Chem. Soc. 110 (1988) 7870–7872.
[40] J. Cavanaugh, M. Rance, J. Magn. Reson. 96 (1992) 670–678.
[41] S. Macura, Y. Huang, D. Suter, R.R. Ernst, J. Magn. Reson. 43 (1981) 259–281.
[42] G. Bodenhausen, D.J. Ruben, Chem. Phys. Lett. 69 (1980) 185–189.
[43] Ē. Kupce, R. Freeman, J. Magn. Reson. Ser. A 117 (1995) 246–256.
[44] A. Bax, M.F. Summers, J. Am. Chem. Soc. 108 (1986) 2093–2094.
[45] R.E. Hurd, J. Magn. Reson. 87 (1990) 422–428.
[46] C.E. Hadden, J. Magn. Reson. 43 (2005) 330–333.
[47] W.P. Neumann, The Organic Chemistry of Tin, Wiley, London, 1970, pp. 211–212.
[48] D. Sun, H. Lennernas, L.S. Welage, J.L. Barnett, C.P. Landowski, D. Foster, D. Fleisher, K.-D. Lee, G.L. Amidon, Pharm. Res. 19 (2002) 1400–1416.
[49] F. Denizot, R. Lang, J. Immunol. Methods 89 (1986) 271–277.
[50] H.-M. Lee, D.S.-H. Chan, F. Yang, H.-Y. Lam, S.-C. Yan, C.-M. Che, D.-L. Ma, C.-H. Leung, Chem. Commun. 46 (2010) 4680–4682.
[51] A.K. Covington, M. Paabo, R.A. Robinson, R.G. Bates, Anal. Chem. 40 (1968) 700–706.
[52] T.P. Lockhart, W.F. Manders, Inorg. Chem. 25 (1986) 892–895.
[53] J. Holeček, M. Nádvorník, K. Handlíř, A. Lyčka, J. Organomet. Chem. 315 (1986) 299–308.
[54] N. Bertazzi, G. Casella, P. D'Agati, T. Fiore, C. Mansueto, V. Mansueto, C. Pellerito, L. Pellerito, M. Scopelliti, Appl. Organomet. Chem. 22 (2008) 389–396.
[55] A. Rotondo, G. Bruno, M. Cusumano, E. Rotondo, Inorg. Chim. Acta 362 (2009) 4767–4773.
[56] A. Rotondo, G. Bruno, G. Brancatelli, F. Nicolò, D. Armentano, Inorg. Chim. Acta 362 (2009) 247–252.
[57] G. Ruisi, L. Canfora, G. Bruno, A. Rotondo, T.F. Mastropietro, E.A. Debbia, M.A. Girasolo, B. Megna, J. Organomet. Chem. 695 (2010) 546–551.
[58] T.S.B. Baul, D. Dutta, A. Duthie, N. Guchhait, B.G.M. Rocha, M.F.C.G. da Silva, R.B. Mokhamatam, N. Raviprakash, S.K. Manna, J. Inorg. Biochem. 166 (2017) 34–48.